

Study a vehicle rollover maneuvers by using LQR active suspension control system

Hamed Soltani¹

¹Department of Automotive Engineering, College of Engineering, Mashhad Branch, Islamic Azad University, Mashhad, IRAN soltani54@yahoo.com

Abstract: This paper presents a control scheme to avoid or minimize the risk of vehicle rollover in certain maneuvers. An active suspension control approach using a linear quadratic regulator with output weighting (LQRY) control design is proposed to control the vehicle. This control scheme is integrated with the full vehicle dynamics simulation program. Motions of the sprung mass have been analyzed. The performance of the active suspension control is demonstrated in simulations. Moreover, the comprehensive vehicle subsystems have been modeled to include active suspensions. The dynamic behavior of a vehicle with active suspension was compared to that of a vehicle without active suspension and it was found that, due to roll angle reduction, the active suspension model was found superior for the purpose of the rollover prevention.

Keywords: Active Suspension Control, Vehicle Rollover, Vehicle Dynamics, Suspension Force.

I. INTRODUCTION

A. Rollover Risk

Traffic crashes are recognized as a major cause of death in the United States claiming approximately 42,000 lives annually¹. One of the leading safety hazards for all classes of light vehicles, especially light trucks (pickups, sport utility vehicles, and vans), is the rollover crash. According to Fatal Accident Reporting System (FARS) data, during the period of 1997 and 2000, an average of 29 percent of all light vehicle fatalities were caused by rollovers. If this threat of rollovers is to be significantly diminished, the research being conducted must focus on creating a more accurate vehicle dynamic model and control scheme. The information such a model could provide would allow for the targeting of specific design issues and improvements thereby minimizing the rollover propensity of the vehicles being manufactured today.

As can be seen in Figure 1a, while only eight percent of light vehicle crashes are statistically defined as rollovers, Figure 1b shows they are responsible for 21 percent of crashes where the occupants are seriously injured. This number jumps to 31 percent when dealing with occupant fatalities, as seen in Figure 1c.

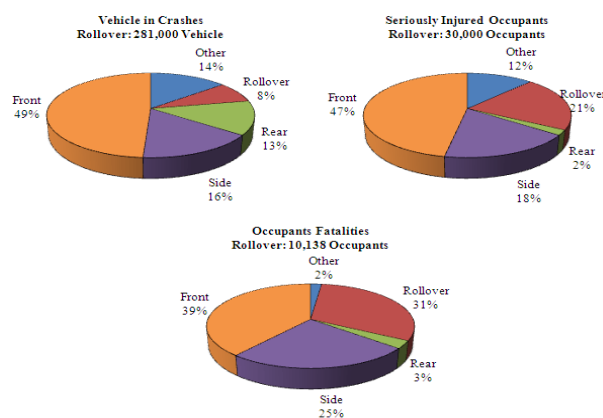


Figure 1: Source: 1997 –2001 NASS-CDS, 2001 FARS

¹ This analysis will be based on 1991 through 2000 data harvested from three sources: the Fatality Analysis Reporting System (FARS), which is an annual census of all fatal motor vehicle crashes occurring in the United States; Federal Highway Administration (FHWA) which provides data on vehicle registration as well as vehicle miles traveled (VMT); and general population data from the United States Census Bureau.

B. Vehicle Handling

The suspension system serves the two-fold purpose of determining ride quality as well as influencing the dynamics of the vehicle (handling performance). In order to successfully manage the performance of the suspension system, variety of dynamic measures such as ride comfort, body motion, suspension travel and vertical force transmitted to the passengers need to be optimized.

So as to improve the suspension outputs such as balance between the ride comfort, handling quality and constraint of suspension travels this study proposes an implementation of dynamic modeling control system to the reduction of vehicle roll angular using a LQRY control design. Multiple actuators and a single goal¹ make LQRY an appropriate selection. This is also a convenient way to optimize the performance vs. actuator use in this particular setting. Another fact to be noted is that modern technology actuator response time is much faster than the roll dynamic. This could cause the time delay control system, another control method, to be neglected.

II. SUSPENSION OVERVIEW

In recent history, passenger car suspension designs have been separated into solid axle and independent suspensions. According to Gillespie [1] nearly all passenger cars and light trucks utilize independent front suspension. Also, the classification of different suspension systems has to be given, according to the levels of their capability for ride comfort and dynamic stability. Before proceeding to the active suspension control systems design the following section classifies and defines them:

A. Passive Suspension System

Conventional passive suspension systems, characteristically containing springs, dampers, and anti-roll bars, are only capable of dissipating energy. In passive systems suspension

Characteristics of stiffness of spring and the damping coefficient of shock absorber are fixed. Hence, these elements have no mechanism for feedback control [2 and 3]. A passive suspension system has been shown in Figure 2.

B. Semi-Active Suspension System

Semi-Active system can only change the viscous damping coefficient of the shock absorber and do not add energy to the suspension system. An important benefit of this type of suspension is that it provides controlled real-time dissipation of energy [3 and 4].

This type of system requires some form of measuring device with a controller board in order to tune the damping properly.

C. Active Suspension System

An active suspension is a critical part of the vehicle, improving comfort and safety [5]. It replaces conventional spring and damper arrangements by using powered actuators. The key characteristic of this system is that it uses an external power source to achieve suspension goal. This extra force compensates road disturbances along with roll and pitch motions of the body. As can be seen in Figure 3, the controller divides the actuator, placed between the car body and the tire axle, based on the designed control law.

The active suspension system controls four actuators at each corner of the car simultaneously. The actuators are mainly powered hydraulically.

In comparison of the three major areas central to the vehicle suspension systems, passive systems can only control the ride height, semi-active systems perform control of ride height and pitching under braking or acceleration and the active suspension systems have power over the springing/damping and hub motions of the vehicle on top of the other areas.

¹ The reduction of the roll angle

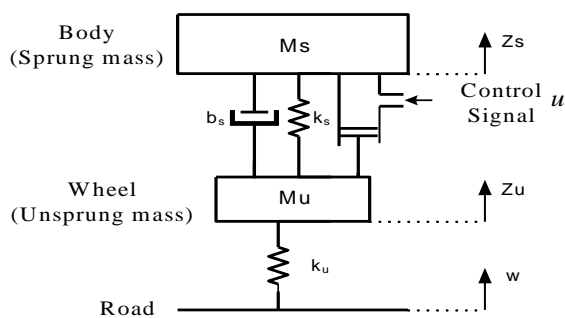


Figure 2: Passive suspension system.

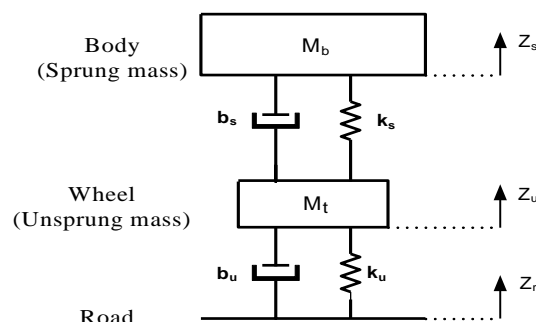


Figure 3: Active suspension system.

III. BACKGROUND

The early work investigating active suspension systems was conducted by Karnoop [7 and 8], Tompsol [8 and 9], and others [5 and 10-12]. Since its initial conception in the late 1960's [13], the field of active suspensions for automotive applications has seen numerous research investigations. These studies have ranged from pure vibration isolation applications [14, 15 and 16], to incorporating handling characteristics into the goal of active suspension control [17]. Chalasani [18 and 19] showed that the active suspension system performed better than the passive system for both quarter car and full-car model.

Various control methods such as optimal state-feedback [14 and 20], backstepping method [21 and 22], fuzzy control [23] and sliding mode control have been proposed in the past years to control the active suspension system.

IV. VEHICLE DYNAMICS SIMULATIONS

There are many advantages of computer models simulation, among which are: an ability to evaluate alternative designs prior to building prototypes, the possibility of studying an existing system's behavior, and observing human behavior as well as hardware components via real time simulation.

Current mechanical multi-body simulation programs such as HVE, VDANL and ADAMS can generate complex nonlinear vehicle models with many degrees of freedom reliably. The use of relatively simple vehicle models in designing vehicle control systems seems a preferable approach. A pertinent example of this is in the attempt to create a model used for the design of the active roll control system of a long combination vehicle, it is only necessary to capture the important yaw and roll dynamics, and not the pitch and bounce motions.

The Center for Intelligent Systems Research (CISR) Vehicle Simulator Laboratory, where this research has been conducted, uses the VDANL program. This program is a non-linear analysis program that comprehensively simulates and evaluates the actions of ground vehicles. This program has been designed to recreate almost anything that can be done in a ground vehicle, including actions such as steady state turn circles, transient lane changes, and braking. Using this software an independent module can be written, compiled, and linked to VDANL when the program begins to run, thus creating a custom version of the program functional for specific internal purposes.

V. THE SUSPENSION MODEL

The full-vehicle suspension system is represented (in Figure 4) as a linearized seven-degree-of-freedom (DOF) system. It consists of a single mass (car body) connected, at each corner, to four unsprung masses (front-left, front-right, rear-left and rear-right wheels). The sprung mass is able to heave, pitch, and roll while the unsprung masses can bounce vertically respectively to the sprung mass. The suspensions between the sprung mass and unsprung masses are modeled as linear viscous dampers and spring elements. Tires are modeled as simple linear springs without damping. Some typical vehicle parameters have been presented as Table 1.

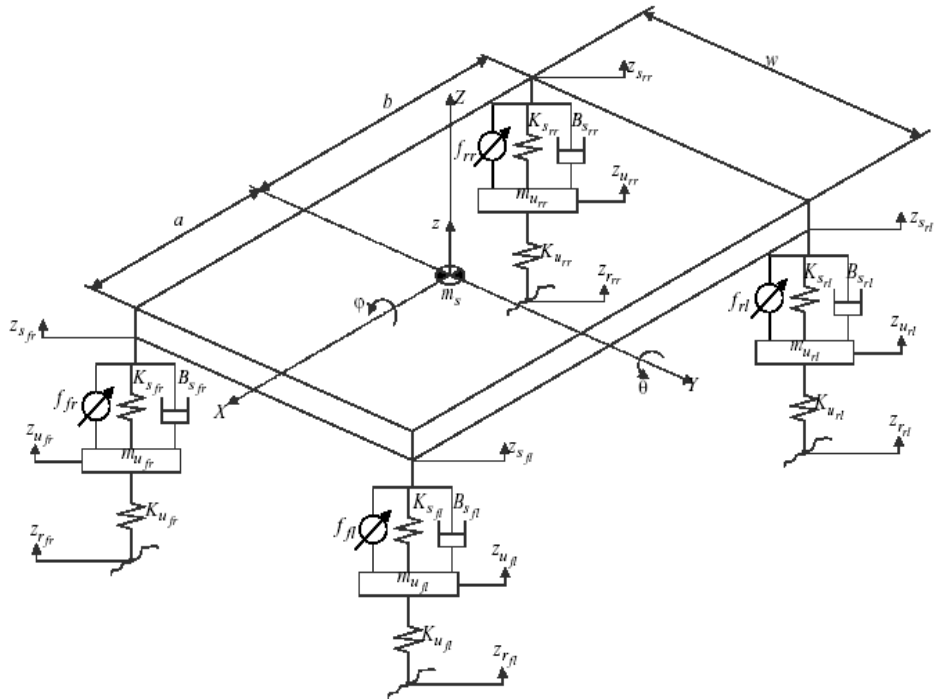


Figure 4: Model of full-vehicle.

The remainder of this study will discuss and overview the concepts of active suspension design as well as the results obtained from the computer simulation with and without an active suspension module.

Table 1: Typical vehicle parameters.

Parameter	m_s (Ib)	m_u (Ib)	B_{sf} (Ib- sec/in)	B_{sr} (Ib- sec/in)	I_{xx} (Ib- sec ² - in)	I_{yy} (Ib- sec ² - in)	a (in)	b (in)	W (in)
Ford Taurus4-Dr (Pas. Car #1)	3248.33	151.99	8.47	6.57	2916.00	20904.00	38.19	70.31	73.10
Dodge Neon4-Dr (Pas. Car#2)	2285.17	168.47	12.00	7.32	2238.17	12259.32	33.03	70.97	67.52
Toyota 4Runner4-Dr (SUV#1)	3355.19	334.93	10.18	7.38	2130.39	18474.80	46.39	58.90	68.18
Ford Explorer 4-Dr (SUV#2)	3947.93	346.91	9.70	7.30	5462.60	31940.20	51.84	60.16	69
Chevrolet S10 (Pickup#1)	2911.14	334.62	11.52	6.80	5829.75	34544.51	49.69	73.21	67.10
Ford F150 (Pick up#2)	3079.56	309.17	10.50	8.13	4527.67	27225.70	45.43	71.37	77.17

According to Leo Davis and et. al. [24] after applying a force-balance analysis to the model in Figure 5, the following equations of motion and state equations are presented as the set of Equations (1) and (2) respectively:

Equations of motion (1)

$$m_s \ddot{z} = -m_s g - (2K_{s_f} + 2K_{s_r})z - (2B_{s_f} + 2B_{s_r})\dot{z} + (2aK_{s_f} - 2bK_{s_r})\theta + (2aB_{s_f} - 2bB_{s_r})\dot{\theta} + K_{s_f} z_{u_{fl}} + B_{s_f} \dot{z}_{u_{fl}} + K_{s_d} z_{u_{fl}} + B_{s_f} \dot{z}_{u_{fr}} + K_{s_r} z_{u_{rl}} + B_{s_r} \dot{z}_{u_{rl}} + K_{s_r} z_{u_{rr}} + B_{s_r} \dot{z}_{u_{rr}} + f_{fl} + f_{fr} + f_{rl} + f_{rr}$$

$$I_{yy} \ddot{\theta} = (2aK_{s_f} - 2bK_{s_r})z + (2aB_{s_f} - 2bB_{s_r})\dot{z} - (2a^2 K_{s_f} + 2b^2 K_{s_r})\theta - (2a^2 B_{s_f} + 2b^2 B_{s_r})\dot{\theta} - aK_{s_f} z_{u_{fl}} - aB_{s_f} \dot{z}_{u_{fl}} - aK_{s_d} z_{u_{fl}} - aB_{s_f} \dot{z}_{u_{fr}} + bK_{s_r} z_{u_{rl}} + bB_{s_r} \dot{z}_{u_{rl}} + bK_{s_r} z_{u_{rr}} + bB_{s_r} \dot{z}_{u_{rr}} - af_{fl} - af_{fr} + bf_{rl} + bf_{rr}$$

$$I_{xx} \ddot{\phi} = -0.25w^2 (2K_{s_f} + 2K_{s_r})\phi - 0.25w^2 (2B_{s_f} + 2B_{s_r})\dot{\phi} + 0.5wK_{s_f} z_{u_{fl}} + 0.5wB_{s_f} \dot{z}_{u_{fl}} - 0.5wK_{s_f} z_{u_{fr}} - 0.5wB_{s_f} \dot{z}_{u_{fr}} + 0.5wK_{s_r} z_{u_{rl}} + 0.5wB_{s_r} \dot{z}_{u_{rl}} - 0.5wK_{s_r} z_{u_{rr}} - 0.5wB_{s_r} \dot{z}_{u_{rr}} + 0.5wf_{fl} - 0.5wf_{fr} + 0.5wf_{rl} - 0.5wf_{rr}$$

$$m_u \ddot{z}_{u_{fl}} = -m_u g + K_{s_f} z + B_{s_f} \dot{z} - aK_{s_f} \theta - aB_{s_f} \dot{\theta} + 0.5wK_{s_f} \phi + 0.5wB_{s_f} \dot{\phi} - (K_{s_f} + K_u)z_{u_{fl}} - B_{s_f} \dot{z}_{u_{fl}} + K_u z_{r_{fl}} - f_{fl}$$

$$m_u \ddot{z}_{u_{fr}} = -m_u g + K_{s_f} z + B_{s_f} \dot{z} - aK_{s_f} \theta - aB_{s_f} \dot{\theta} - 0.5wK_{s_f} \phi - 0.5wB_{s_f} \dot{\phi} - (K_{s_f} + K_u)z_{u_{fr}} - B_{s_f} \dot{z}_{u_{fr}} + K_u z_{r_{fr}} - f_{fr}$$

$$m_u \ddot{z}_{u_{rl}} = -m_u g + K_{s_r} z + B_{s_r} \dot{z} - aK_{s_r} \theta - aB_{s_r} \dot{\theta} + 0.5wK_{s_r} \phi + 0.5wB_{s_r} \dot{\phi} - (K_{s_r} + K_u)z_{u_{rl}} - B_{s_r} \dot{z}_{u_{rl}} + K_u z_{r_{rl}} - f_{rl}$$

$$m_u \ddot{z}_{u_{rr}} = -m_u g + K_{s_r} z + B_{s_r} \dot{z} + bK_{s_r} \theta + bB_{s_r} \dot{\theta} - 0.5wK_{s_r} \phi - 0.5wB_{s_r} \dot{\phi} - (K_{s_r} + K_u)z_{u_{rr}} - B_{s_r} \dot{z}_{u_{rr}} + K_u z_{r_{rr}} - f_{rr}$$

The system states are assigned as

- | | | | |
|----------------------|--|-----------------------------|--|
| $x_1 = z$ | heave position (ride height of sprung mass) | $x_8 = \dot{z}_{u_{fl}}$ | front-left wheel unsprung mass velocity |
| $x_2 = \dot{z}$ | heave velocity (payload velocity of sprung mass) | $x_9 = z_{u_{fr}}$ | front-right wheel unsprung mass height |
| $x_3 = \theta$ | pitch angle | $x_{10} = \dot{z}_{u_{fr}}$ | front-right wheel unsprung mass velocity |
| $x_4 = \dot{\theta}$ | pitch angular velocity | $x_{11} = z_{u_{rl}}$ | rear-left wheel unsprung mass height |
| $x_5 = \phi$ | roll angle | $x_{12} = \dot{z}_{u_{rl}}$ | rear-left wheel unsprung mass velocity |
| $x_6 = \dot{\phi}$ | roll angular velocity | $x_{13} = z_{u_{rr}}$ | rear-right wheel unsprung mass height |
| $x_7 = z_{u_{fl}}$ | front-left wheel unsprung mass height | $x_{14} = \dot{z}_{u_{rr}}$ | rear-right wheel unsprung mass velocity |

State Equations

(2)

$$\dot{x}_1 = x_2$$

$$\dot{x}_2 = \frac{(2K_{sf} + 2K_{sr})}{m_s} x_1 - \frac{(2B_{sf} + 2B_{sr})}{m_s} x_2 + \frac{(2aK_{sf} - 2bK_{sr})}{m} x_3 + \frac{(2aB_{sf} - 2bB_{sr})}{m_s} x_4 + \frac{K_{sf}}{m_s} x_7 + \frac{B_{sf}}{m_s} x_9 + \frac{B_{sf}}{m_s} x_{10} + \frac{K_{sr}}{m_s} x_{11} + \frac{B_{sr}}{m_s} x_{12} + \frac{K_{sr}}{m_s} x_{13} + \frac{B_{sr}}{m_s} x_{14} + \frac{1}{m_s} f_{fl} + \frac{1}{m_s} f_{fr} + \frac{1}{m_s} f_{rl} + \frac{1}{m_s} f_{rr}$$

$$\dot{x}_3 = x_4$$

$$\dot{x}_4 = \frac{(2aK_{sf} - 2bK_{sr})}{I_{yy}} x_1 + \frac{(2aB_{sf} - 2bB_{sr})}{I_{yy}} x_2 - \frac{(2a^2K_{sf} + 2b^2K_{sr})}{I_{yy}} x_3 - \frac{(2a^2B_{sf} + 2b^2B_{sr})}{I_{yy}} x_4 - \frac{aK}{I_{yy}} x_8 - \frac{aB_{sf}}{I_{yy}} x_9 - \frac{aK_{sf}}{I_{yy}} x_{10} + \frac{bK_{sr}}{I_{yy}} x_{11} + \frac{bB_{sr}}{I_{yy}} x_{12} + \frac{bK_{sf}}{I_{yy}} x_{13} + \frac{bB_{sf}}{I_{yy}} x_{14} - \frac{a}{I_{yy}} f_{fl} - \frac{a}{I_{yy}} f_{fr} + \dots + \frac{b}{I_{yy}} f_{rl} + \frac{b}{I_{yy}} f_{rr}$$

$$\dot{x}_5 = x_6$$

$$\dot{x}_6 = \frac{w^2(2K_{sf} + 2K_{sr})}{4I_{xx}} x_5 - \frac{w^2(2B_{sf} - 2B_{sr})}{4I_{xx}} x_6 + \frac{wK_{sf}}{2I_{xx}} x_7 + \frac{wK_{sr}}{2I_{xx}} x_8 - \frac{wK_{sf}}{2I_{xx}} x_9 - \frac{wB_{sf}}{2I_{xx}} x_{10} + \dots + \frac{wK_{sr}}{2I_{xx}} x_{11} + \frac{wB_{sr}}{2I_{xx}} x_{12} - \frac{wK_{sr}}{2I_{xx}} x_{13} - \frac{wB_{sr}}{2I_{xx}} x_{14} + \frac{w}{2I_{xx}} f_{fl} - \frac{w}{2I_{xx}} f_{fr} + \frac{w}{2I_{xx}} f_{rl} - \frac{w}{2I_{xx}} f_{rr}$$

$$\dot{x}_7 = x_8$$

$$\dot{x}_8 = \frac{K_{sf}}{m_u} x_1 + \frac{B_{sf}}{m_u} x_2 - \frac{aK_{sf}}{m_u} x_3 - \frac{aB_{sf}}{m_u} x_4 + \frac{wK_{sf}}{2m_u} x_5 + \frac{wB_{sf}}{2m_u} x_6 - \frac{(K_{sf} + K_u)}{m_u} x_7 - \frac{B_{sf}}{m_u} x_8 - \frac{1}{m_u} f_{fl}$$

$$\dot{x}_9 = x_{10}$$

$$\dot{x}_{10} = \frac{K_{sf}}{m_u} x_1 + \frac{B_{sf}}{m_u} x_2 - \frac{aK_{sf}}{m_u} x_3 - \frac{aB_{sf}}{m_u} x_4 - \frac{wK_{sf}}{2m_u} x_5 - \frac{wB_{sf}}{2m_u} x_6 - \frac{(K_{sf} + K_u)}{m_u} x_7 - \frac{B_{sf}}{m_u} x_{10} - \frac{1}{m_u} f_{fl}$$

$$\dot{x}_{11} = x_{12}$$

$$\dot{x}_{12} = \frac{K_{sr}}{m_u} x_1 + \frac{B_{sr}}{m_u} x_2 + \frac{bK_{sr}}{m_u} x_3 + \frac{bB_{sr}}{m_u} x_4 + \frac{wK_{sr}}{2m_u} x_5 + \frac{wB_{sr}}{2m_u} x_6 - \frac{(K_{sr} + K_u)}{m_u} x_{11} - \frac{B_{sr}}{m_u} x_{12} - \frac{1}{m_u} f_{fr}$$

$$\dot{x}_{13} = x_{14}$$

The State Space Equations in matrix form are given by:

$$\dot{x}(t) = Ax(t) + Bf(t) \tag{3}$$

$$y(t) = Cx(t) \tag{4}$$

With the control input $f(t)$ defined as the force generated at the front-left, front-right, rear-left and rear-right suspensions respectively as $f(t) = [f_{fl}(t) \ f_{fr}(t) \ f_{rl}(t) \ f_{rr}(t)]^T$. The output $y(t)$ is selected for specific performance-analysis objectives (roll angle and roll reduction).

The constant A, B, and C matrices have been defined as a set of Equations (5).

Where

m_s = spring mass

m_u = un-sprung mass

I_{yy} = pitch axis moment of inertia

a = length between front of vehicle and C.G of sprung mass

B_{sr} = front suspension viscous

B_{ur} = rear suspension viscous

I_{xx} = roll axis moment of inertia

W = width of sprung mass

b = length between rear of vehicle and C.G of sprung mass

$$A = \begin{bmatrix} \frac{0}{(2K_{sf}+2K_{sr})} & \frac{1}{(2B_{sf}+2B_{sr})} & \frac{0}{(2aK_{sf}-2bK_{sr})} & \frac{0}{(2aB_{sf}-2bB_{sr})} & \frac{0}{K_{sf}} & \frac{0}{B_{sf}} & \frac{0}{K_{sf}} & \frac{0}{B_{sf}} & \frac{0}{K_{sr}} & \frac{0}{B_{sr}} & \frac{0}{K_{sr}} & \frac{0}{B_{sr}} & 0 & 0 \\ m_s & m_s & m_s & m_s & m_s & m_s & m_s & m_s & m_s & m_s & m_s & m_s & 0 & 0 \\ \frac{0}{(2aK_{sf}-2bK_{sr})} & \frac{0}{(2aB_{sf}-2bB_{sr})} & \frac{0}{(2a^2K_{sf}+2b^2K_{sr})} & \frac{1}{(2a^2B_{sf}+2b^2B_{sr})} & \frac{0}{aK_{sf}} & \frac{0}{aB_{sf}} & \frac{0}{aK_{sf}} & \frac{0}{aB_{sf}} & \frac{0}{bK_{sf}} & \frac{0}{bB_{sf}} & \frac{0}{bK_{sf}} & \frac{0}{bB_{sf}} & 0 & 0 \\ \frac{I_{xx}}{I_{yy}} & \frac{I_{yy}}{I_{xx}} & \frac{I_{yy}}{I_{yy}} & \frac{I_{yy}}{I_{yy}} & \frac{I_{yy}}{I_{yy}} & \frac{I_{yy}}{I_{yy}} & \frac{I_{yy}}{I_{yy}} & \frac{I_{yy}}{I_{yy}} & \frac{I_{yy}}{I_{yy}} & \frac{I_{yy}}{I_{yy}} & \frac{I_{yy}}{I_{yy}} & \frac{I_{yy}}{I_{yy}} & \frac{I_{yy}}{I_{yy}} & \frac{I_{yy}}{I_{yy}} \\ \frac{0}{w^2(2K_{sf}+2K_{sr})} & \frac{0}{w^2(2B_{sf}+2B_{sr})} & \frac{0}{wK_{sf}} & \frac{0}{wB_{sf}} & \frac{0}{wK_{sf}} & \frac{0}{wB_{sf}} & \frac{0}{wK_{sr}} & \frac{0}{wB_{sr}} & \frac{0}{wK_{sr}} & \frac{0}{wB_{sr}} & \frac{0}{wK_{sr}} & \frac{0}{wB_{sr}} & 0 & 0 \\ \frac{4I_{yy}}{4I_{xx}} & \frac{4I_{xx}}{4I_{yy}} & \frac{2I_{xx}}{2I_{xx}} & \frac{2I_{xx}}{2I_{xx}} & \frac{2I_{xx}}{2I_{xx}} & \frac{2I_{xx}}{2I_{xx}} & \frac{2I_{xx}}{2I_{xx}} & \frac{2I_{xx}}{2I_{xx}} & \frac{2I_{xx}}{2I_{xx}} & \frac{2I_{xx}}{2I_{xx}} & \frac{2I_{xx}}{2I_{xx}} & \frac{2I_{xx}}{2I_{xx}} & 0 & 0 \\ \frac{0}{K_{sf}} & \frac{0}{B_{sf}} & \frac{0}{aK_{sf}} & \frac{0}{aB_{sf}} & \frac{0}{wK_{sf}} & \frac{0}{wB_{sf}} & \frac{0}{wK_{sf}} & \frac{0}{wB_{sf}} & \frac{0}{(K_{sf}+K_u)} & \frac{0}{B_{sf}} & \frac{0}{B_{sf}} & \frac{0}{B_{sf}} & 0 & 0 \\ m_u & m_u & m_u & m_u & 2m_u & 2m_u & m_u & m_u & m_u & m_u & m_u & m_u & 0 & 0 \\ \frac{0}{K_{sf}} & \frac{0}{B_{sf}} & \frac{0}{aK_{sf}} & \frac{0}{aB_{sf}} & \frac{0}{wK_{sf}} & \frac{0}{wB_{sf}} & \frac{0}{wK_{sf}} & \frac{0}{wB_{sf}} & \frac{0}{(K_{sf}+K_u)} & \frac{0}{B_{sf}} & \frac{0}{B_{sf}} & \frac{0}{B_{sf}} & 0 & 0 \\ m_u & m_u & m_u & m_u & 2m_u & 2m_u & m_u & m_u & m_u & m_u & m_u & m_u & 0 & 0 \\ \frac{0}{K_{sr}} & \frac{0}{B_{sr}} & \frac{0}{bK_{sr}} & \frac{0}{bB_{sr}} & \frac{0}{wK_{sr}} & \frac{0}{wB_{sr}} & \frac{0}{wK_{sr}} & \frac{0}{wB_{sr}} & \frac{0}{(K_{sr}+K_u)} & \frac{0}{B_{sr}} & \frac{0}{B_{sr}} & \frac{0}{B_{sr}} & 0 & 0 \\ m_u & m_u & m_u & m_u & 2m_u & 2m_u & m_u & m_u & m_u & m_u & m_u & m_u & 0 & 0 \\ \frac{0}{K_{sr}} & \frac{0}{B_{sr}} & \frac{0}{bK_{sr}} & \frac{0}{bB_{sr}} & \frac{0}{wK_{sr}} & \frac{0}{wB_{sr}} & \frac{0}{wK_{sr}} & \frac{0}{wB_{sr}} & \frac{0}{(K_{sr}+K_u)} & \frac{0}{B_{sr}} & \frac{0}{B_{sr}} & \frac{0}{B_{sr}} & 0 & 0 \\ m_u & m_u & m_u & m_u & 2m_u & 2m_u & m_u & m_u & m_u & m_u & m_u & m_u & 0 & 0 \\ \frac{0}{K_{sr}} & \frac{0}{B_{sr}} & \frac{0}{bK_{sr}} & \frac{0}{bB_{sr}} & \frac{0}{wK_{sr}} & \frac{0}{wB_{sr}} & \frac{0}{wK_{sr}} & \frac{0}{wB_{sr}} & \frac{0}{(K_{sr}+K_u)} & \frac{0}{B_{sr}} & \frac{0}{B_{sr}} & \frac{0}{B_{sr}} & 0 & 0 \\ m_u & m_u & m_u & m_u & 2m_u & 2m_u & m_u & m_u & m_u & m_u & m_u & m_u & 0 & 0 \end{bmatrix}$$

$$B = \begin{bmatrix} \frac{0}{1} & \frac{0}{1} & \frac{0}{1} & \frac{0}{1} \\ \frac{m_s}{a} & \frac{m_s}{a} & \frac{m_s}{b} & \frac{m_s}{b} \\ \frac{I_{yy}}{w} & \frac{I_{yy}}{w} & \frac{I_{yy}}{w} & \frac{I_{yy}}{w} \\ \frac{0}{2I_{xx}} & \frac{0}{2I_{xx}} & \frac{0}{2I_{xx}} & \frac{0}{2I_{xx}} \\ \frac{0}{1} & \frac{0}{1} & \frac{0}{1} & \frac{0}{1} \\ \frac{m_u}{m_u} & \frac{0}{m_u} & \frac{0}{m_u} & \frac{0}{m_u} \\ \frac{0}{1} & \frac{0}{1} & \frac{0}{1} & \frac{0}{1} \\ \frac{0}{m_u} & \frac{0}{m_u} & \frac{0}{m_u} & \frac{0}{m_u} \\ \frac{0}{1} & \frac{0}{1} & \frac{0}{1} & \frac{0}{1} \\ \frac{0}{m_u} & \frac{0}{m_u} & \frac{0}{m_u} & \frac{0}{m_u} \\ \frac{0}{1} & \frac{0}{1} & \frac{0}{1} & \frac{0}{1} \\ \frac{0}{m_u} & \frac{0}{m_u} & \frac{0}{m_u} & \frac{0}{m_u} \end{bmatrix}$$

$$C = \begin{bmatrix} 0 & 0 & 0 & 0 & 1 & 0 & 0 & 0 & 0 & 0 & 0 & 0 & 0 & 0 \\ 0 & 0 & 0 & 0 & 0 & 1 & 0 & 0 & 0 & 0 & 0 & 0 & 0 & 0 \end{bmatrix}$$

VI. SUSPENSION FORCE DEVELOPMENT

Before adding the active suspension module to the program, the suspension forces that the program uses for vehicle modeling must be examined. At that point, a distinct active control force can be defined, for our purposes, and added to the available tire forces (suspension forces). This distinct active control force can then be assumed as an actuator force.

There are several factors that influence suspension force as it acts on the sprung and unsprung masses. These forces include, but are not limited to, a comparison of differing suspensions, relative roll angle, and squat/lift reactions. In order to create applicability to a broad array of suspension types, the force reactions of each wheel have been modified in such a way that their equivalent force will act at the track width.

This includes effects from suspension spring load, shock absorber damping, auxiliary roll stiffness, bump stop forces, and squat/lift forces from suspension geometry reactions as Figure 5 demonstrate [25].

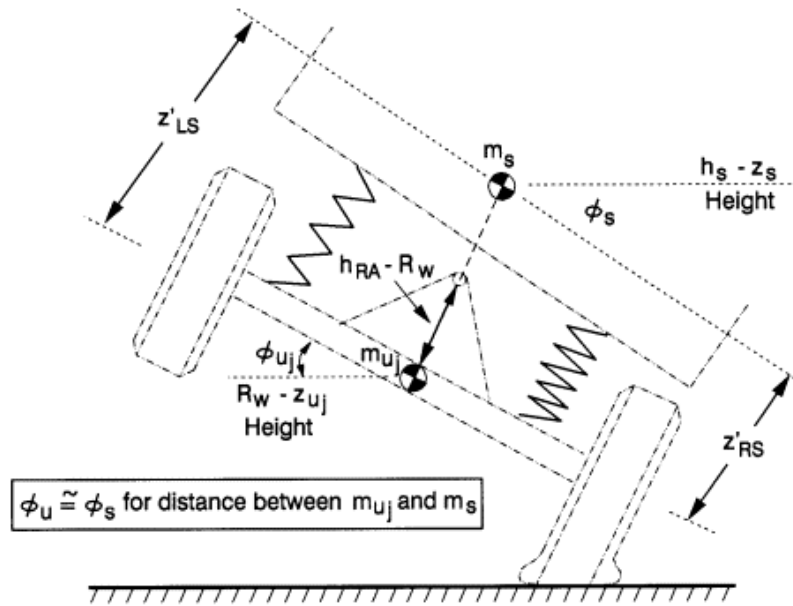


Figure 5: Change in suspension spring length.

Equations (6 to 15) provide a typical tire force processing for a typical passenger car.

$$F_{SLj} = F_{SLj0} - Z_{SLj} K_{Sj} - \dot{Z}_{SLj} K_{SDj} + \frac{(\phi_s - \phi_{uj}) K_{TSj}}{T_j} + F_{BSLj} + F_{SQLj} \quad (6)$$

$$F_{SRj} = F_{SRj0} - Z_{SRj} K_{Sj} - \dot{Z}_{SRj} K_{SDj} + \frac{(\phi_s - \phi_{uj}) K_{TSj}}{T_j} + F_{BSRj} + F_{SORj} \quad (7)$$

Where

- F_{Sij} =suspension force (lb) ϕ_s =sprung mass roll angle (rad)
- F_{BSij} =bump stop force (lb) ϕ_{Uj} =unsprung mass roll angle (rad)
- T_j =track width, j = F, R

K_{SLF} is the linear change in vertical force with lateral force, and is related to roll center form

$$K_{SLF} = \frac{2 \cdot H_{RollCenter}}{TrackWidth}$$

Where the roll center height, $H_{RollCenter}$, is positive if it is above the ground. The roll center is computed as $\frac{\partial F_z}{\partial F_y} \frac{T}{2}$, which is the slope of the vertical force reaction to lateral force multiplied by half the track width.

$$K_{SLF} = 2 \times 5.12/61.5 = 0.17 \quad K_{SLR} = 2 \times 4.35/60.5 = 0.14$$

K_{SF} =front suspension spring rate equivalent at each wheel , 1818 (lbs/ft)

K_{SR} =front suspension spring rate equivalent at each wheel , 1200 (lbs/ft)

K_{SDj} =suspension damping rate equivalent at each wheel (lbs-sec/ft)

K_{TSj} =auxiliary torsional roll stiffness per axle, (normally negative) (ft-lbs/rad)

and

$$F_{SQiF} = \left[K_{SLF} + \frac{Z_{SIF}}{LSAF} \right] F_{YiF}, i = L, R$$

Where F_{SQiF} is front wheel vertical force due to lateral force (Ib), F_{yiF} (Ib)

Z_s =sprung mass vertical deflection (ft) Z_{Uj} =unsprung mass vertical deflection (ft)
 \dot{Z}_s =sprung mass vertical velocity (ft/sec) \dot{Z}_{Uj} =unsprung mass vertical velocity (ft/sec)

In the prior suspension force equations, the values Z_{Sij} and \dot{Z}_{Sij} need to be calculated. These equations define the change in spring length, starting from what the spring length is at curb load, F_{Sij0} .

$$Z_{SLF} = \frac{h_s - RR_F + Z_{UF} - Z_s}{\cos \phi_s} - h_s + RR_F + a\theta + (\phi_s - \phi_{UF}) \frac{T_F}{2} \tag{8}$$

$$Z_{SRF} = \frac{h_s - RR_F + Z_{UF} - Z_s}{\cos \phi_s} - h_s + RR_F + a\theta - (\phi_s - \phi_{UF}) \frac{T_F}{2} \tag{9}$$

$$Z_{SLR} = \frac{h_s - RR_R + Z_{UR} - Z_s}{\cos \phi_s} - h_s + RR_R - b\theta + (\phi_s - \phi_{UR}) \frac{T_R}{2} \tag{10}$$

$$Z_{SRR} = \frac{h_s - RR_R + Z_{UR} - Z_s}{\cos \phi_s} - h_s + RR_R - b\theta - (\phi_s - \phi_{UR}) \frac{T_R}{2} \tag{11}$$

$$\dot{Z}_{SLF} = (h_s - RR_F + Z_{UF} - Z_s) \frac{\tan(\phi_s)}{\cos(\phi_s)} \dot{\phi}_s + \frac{\dot{Z}_{UF} - \dot{Z}_s}{\cos(\phi_s)} + a\dot{\theta} + (\dot{\phi}_s - \dot{\phi}_{UF}) \frac{T_F}{2} \tag{12}$$

$$\dot{Z}_{SRF} = (h_s - RR_F + Z_{UF} - Z_s) \frac{\tan(\phi_s)}{\cos(\phi_s)} \dot{\phi}_s + \frac{\dot{Z}_{UF} - \dot{Z}_s}{\cos(\phi_s)} + a\dot{\theta} - (\dot{\phi}_s - \dot{\phi}_{UF}) \frac{T_F}{2} \tag{13}$$

$$\dot{Z}_{SLR} = (h_s - RR_R + Z_{UR} - Z_s) \frac{\tan(\phi_s)}{\cos(\phi_s)} \dot{\phi}_s + \frac{\dot{Z}_{UR} - \dot{Z}_s}{\cos(\phi_s)} - b\dot{\theta} + (\dot{\phi}_s - \dot{\phi}_{UR}) \frac{T_R}{2} \tag{14}$$

$$\dot{Z}_{SRR} = (h_s - RR_R + Z_{UR} - Z_s) \frac{\tan(\phi_s)}{\cos(\phi_s)} \dot{\phi}_s + \frac{\dot{Z}_{UR} - \dot{Z}_s}{\cos(\phi_s)} - b\dot{\theta} - (\dot{\phi}_s - \dot{\phi}_{UR}) \frac{T_R}{2} \tag{15}$$

Where

RR_j =average axle rolling radius (ft) h_s =sprung mass center of gravity height (ft)
 a =distance form ms C.G. to front axle θ_s =pitch angle (rad)
 b =distance form ms C.G. to rear axle $\dot{\theta}_s$ =pitch velocity (rad/sec)

VII. CONTROL STRATEGIES

The controller design, which utilizes optimal control, will change the feedback gains according to the identified parameters when the active systems are operating. The controller is selected as LQRY. Using equation (3)

$$\dot{x}(t) = Ax(t) + Bf(t)$$

$$u(t) = -K x(t) \tag{16}$$

The feedback gain matrix K is obtained by the optimal control theory stated as follows:

The performance index that minimizes the quadratic cost function with output weighting

$$J(u) = \int (y^T Q y + u^T R u + 2 \times y^T N u) dt \tag{17}$$

(or its discrete counterpart). The function LQRY is equivalent to LQR with weighting matrices:

$$\begin{bmatrix} \bar{Q} & \bar{N} \\ \bar{N}^T & \bar{R} \end{bmatrix} = \begin{bmatrix} C^T & O \\ D^T & I \end{bmatrix} \begin{bmatrix} Q & N \\ N^T & R \end{bmatrix} \begin{bmatrix} C & D \\ 0 & I \end{bmatrix} \tag{18}$$

[K,S,e] = lqry (sys,Q,R,N) returns the optimal gain matrix K, the Riccati solution S, and the closed-loop eigenvalues $e = \text{eig}(A-B*K)$. The state-space model system specifies the continuous- or discrete-time plant data (A, B, C, D). The default value N=0 is assumed when N is omitted [26][27][28].

VIII. IMPLEMENTATION METHOD

The optimal control strategy and the suspension model have been programmed in Visual Basic to be integrated with the VDANL vehicle dynamics model. Break points which lead to new external module allow the user to specify at what exact point in the program any given code will be implemented.

Control laws that can change the suspension forces based on the varying states of the vehicle have been ascertained. During the simulation's initial set up, the Suspension Break Point will be activated. Once the simulation begins to run, the values for the suspension forces (VD.FSLF, VD.FSLR, VD.FSRF, and VD.FSRR) are computed. The program will then turn control over to the suspension module. Inside the module, the vehicle's current dynamics are used to calculate a new set of suspension forces. The suspension forces determined by computer simulation will then be re-assigned with those calculated in the module. All subsequent calculations within VDNAL will then use these new suspension forces. This process continues for each time step of the program.

The latest version of VDANL (6.x) has replaced the numbers previous versions associated with the breakpoints with methods in the Active XDLL. The Visual Basic program lists suspension modules designed for active suspension by the author and includes suspension parameters as well as their descriptions. This list has been provided in Appendix A.

IX. SIMULATION RESULTS

The results of the simulation comparison with and without active suspension have been illustrated in Table 2. The last column of this table shows with the help of active suspension four out of six vehicles have been prevented from tire lift-off. The roll angle variations between vehicles with and without active suspension have been demonstrated in the following roll angle versus time figures (Figures 6, 9 and 12). It is important to note that the research conducted used two-turn, un-tripped, and on-road maneuvers. When taking the data into account, it becomes evident that there is an average reduction of 0.1 radian (20%) roll angle at the point of lift-off. Because this translates into a less severe roll angle, the control of the vehicle is less compromised, causing enhanced driver control. This effect becomes pivotal in constructing a helpful system with regards to rollover prevention in cases involving turning maneuvers.

A vehicle with active suspension experiences a 20 percent decrease in peak tire force at the point of lift-off. This reduction enhances vehicle control and handling, and in the case of this specific study, aids in the prevention of lift-off, making an active suspension far superior to an inactive one.

Table 2: Simulation comparison of vehicles with and without active suspension.

Vehicle Number	Active Suspension	Roll Angle	Tire Force Right Rear	Tire Force Right Front	Tire Force Left Rear	Tire Force Left Front	Comparison Lift-off
PC#1	Without	-0.36	0.00	0.00	814.708	1374.80	Yes
	With	-0.21	61.44	140.92	801.32	1279.576	No
PC#2	Without	-0.35	75.06	0.00	978.57	1259.99	No
	With	-0.29	249.81	150.31	882.89	1091.65	No
SUV#1	Without	-0.64	83.36	7.66	949.23	1615.66	No
	With	-0.53	113.01	75.22	943.00	1600.24	No
SUV#2	Without	-0.35	0.00	0.00	658.11	1383.53	Yes
	With	-0.20	61.24	92.47	557.43	1248.87	No
PT#1	Without	-0.77	0.00	0.00	3814.65	3162.87	Yes
	With	-0.64	300.86	781.85	4217.24	2576.14	No
PT#2	Without	-0.53	0.00	0.00	3333.46	2252.34	Yes
	With	-0.48	486.47	779.98	2704.22	1561/56	No

Figure 6 shows that during the simulation involving passenger car #1, the point of lift-off occurred at about 37 seconds. The roll angle variation for vehicles with and without active suspension at this point is 41.25 %. This aids roll angle reduction when the vehicle reaches the lift-off threshold.

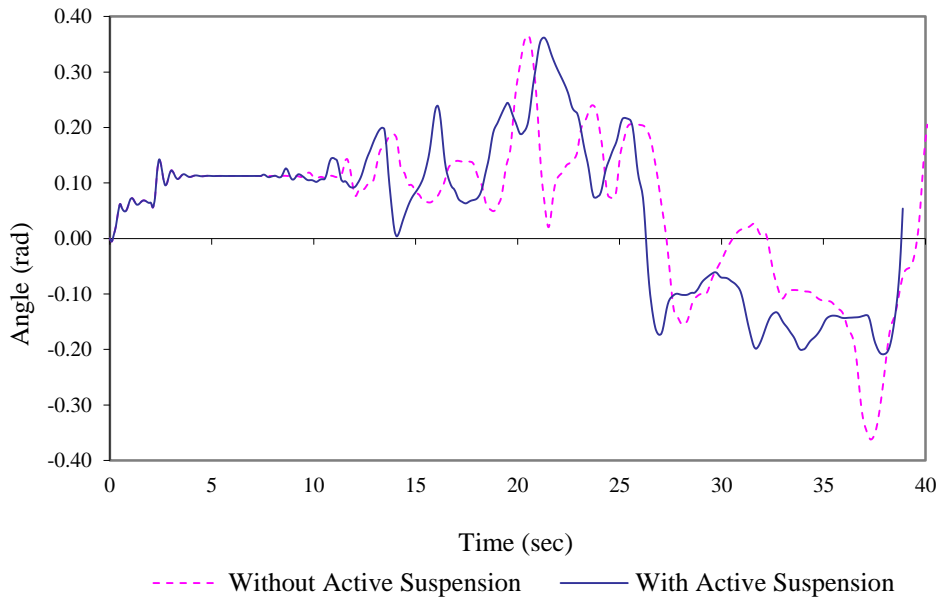


Figure 6: Sprung mass roll angle with and without active suspension Ford Taurus 4-Dr, Passenger Car #1.

Figure 7 demonstrated that at the point of lift-off, in the model without active suspension, tire forces under the right rear (RR) and right front (RF) tires went to zero. When the same tires were evaluated in models with active suspension, however, it was found that some tire forces remained (Figure 8). This residual force prevented lift-off.

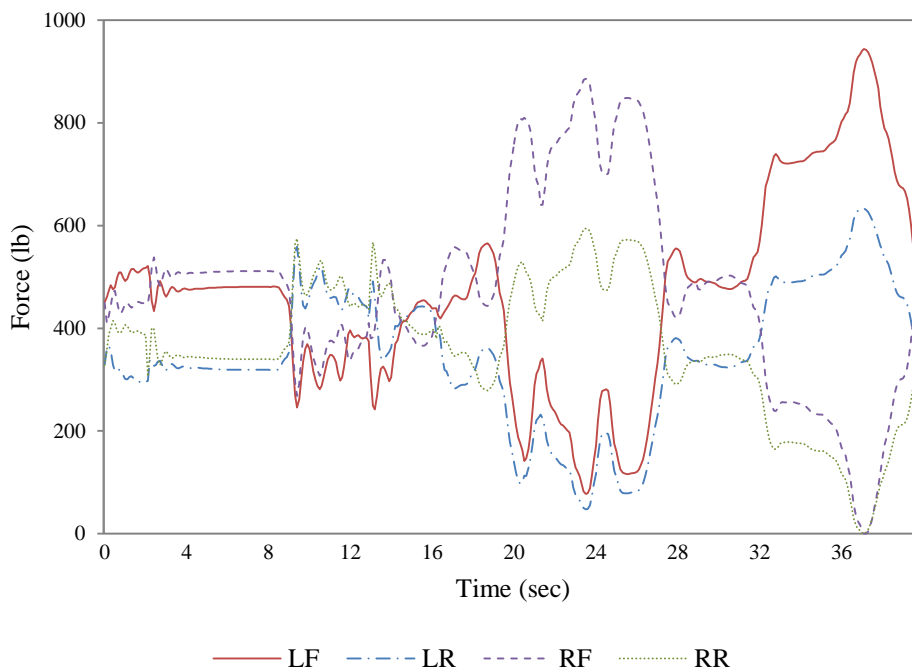


Figure 7: Left Rear (LR), Left Front (LF), Right Rear (RR), and Right Front (RF) tire forces without active, suspension Ford Taurus 4-Dr, Passenger Car #1.

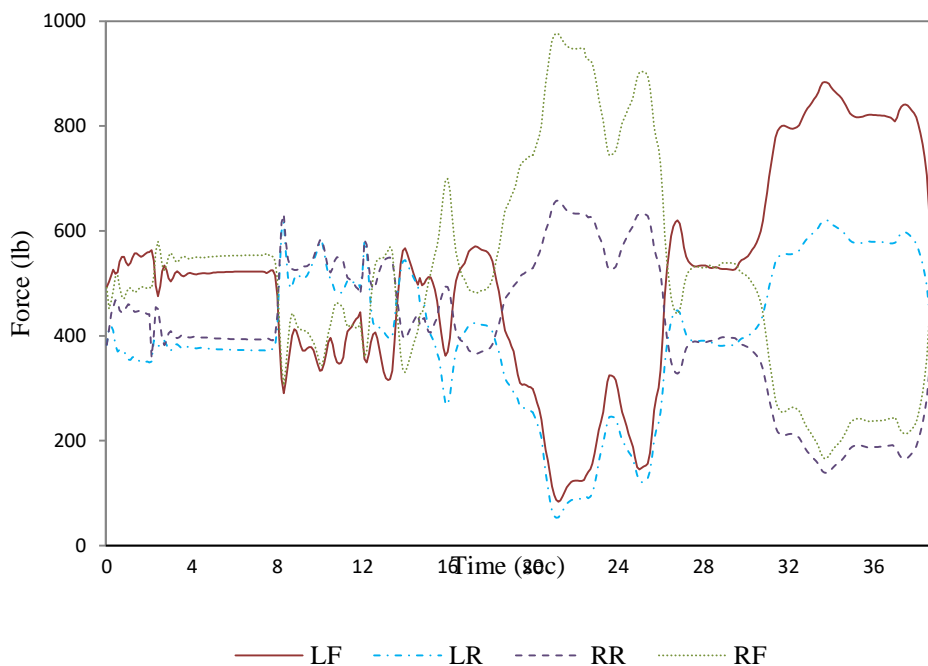


Figure 8: Left Rear (LR), Left Front (LF), Right Rear (RR), and Right Front (RF) tire forces with active suspension Ford Taurus 4-Dr, Passenger Car #1.

Figure 9 shows that during the simulation involving SUV #2, the point of lift-off occurred at about 42 seconds. The roll angle variation for vehicles with and without active suspension at this point is 40%. This aids roll angle reduction when the vehicle reaches the lift-off threshold.

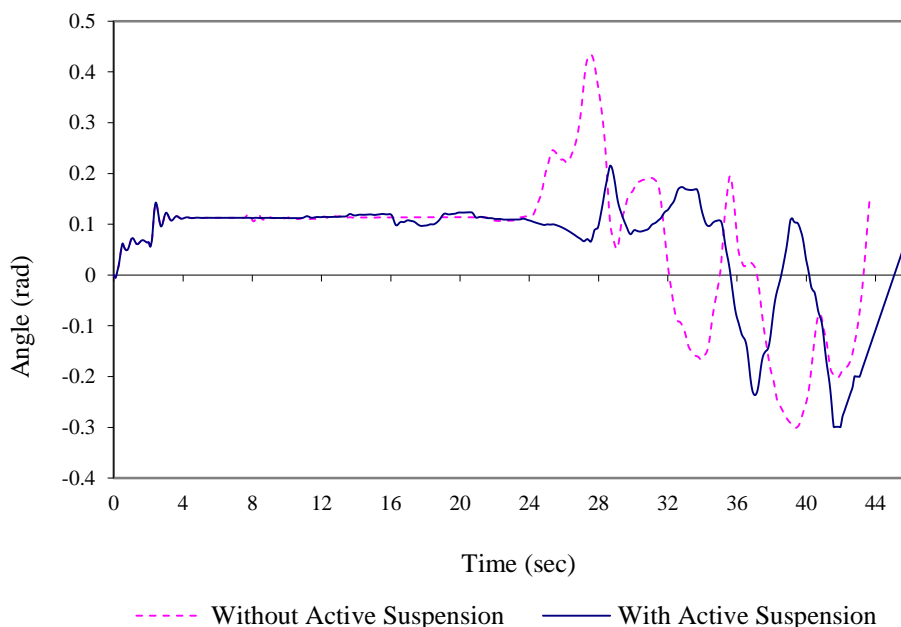


Figure 9: Sprung mass roll angle with and without active suspension Ford Explorer 4-Dr, SUV # 2.

Figure 10 demonstrated that at the point of lift-off, in the model without active suspension, tire forces under the right rear (RR) and right front (RF) tires went to zero. When the same tires were evaluated in models with active suspension, however, it was found that some tire forces remained (Figure 11). This residual force prevented lift-off.

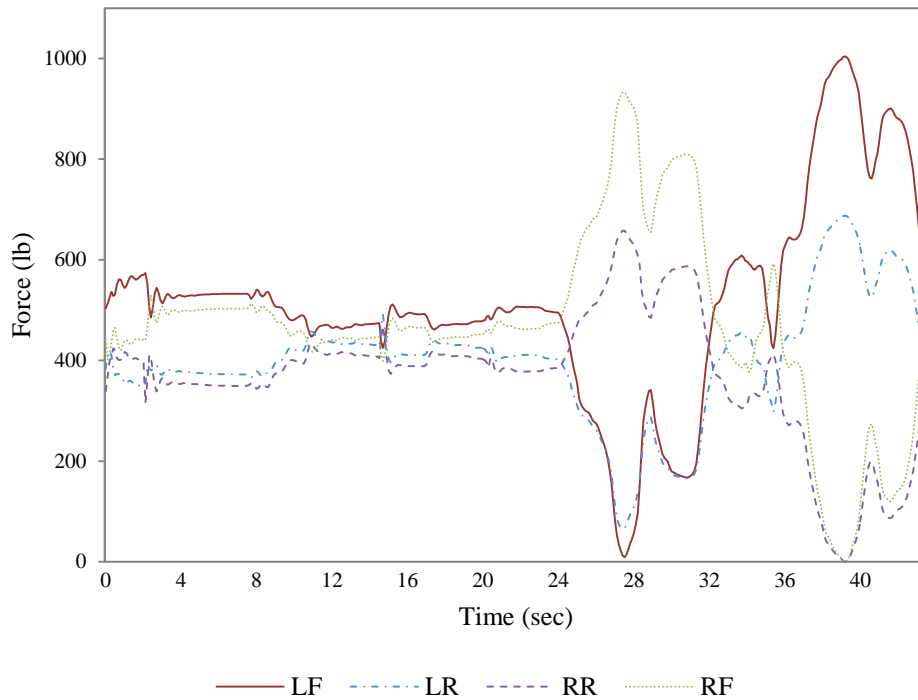


Figure 10: Left Rear (LR), Left Front (LF), Right Rear (RR), and Right Front (RF) tire forces without active suspension, Ford Explorer 4-Dr, SUV # 2.

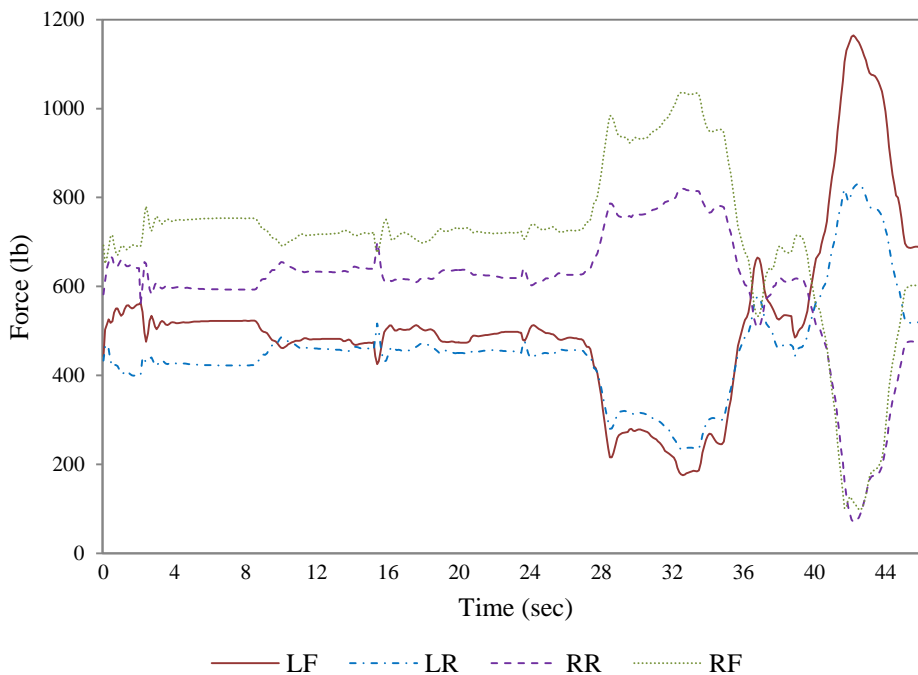


Figure 11: Left Rear (LR), Left Front (LF), Right Rear (RR), and Right Front (RF) tire forces with active suspension, Ford Explorer 4-Dr, SUV # 2.

Figure 12 shows that during the simulation involving Pickup#1, the point of lift-off occurred at about 40 seconds. The roll angle variation for vehicles with and without active suspension at this point is 21.87 %. This aids roll angle reduction when the vehicle reaches the lift-off threshold.

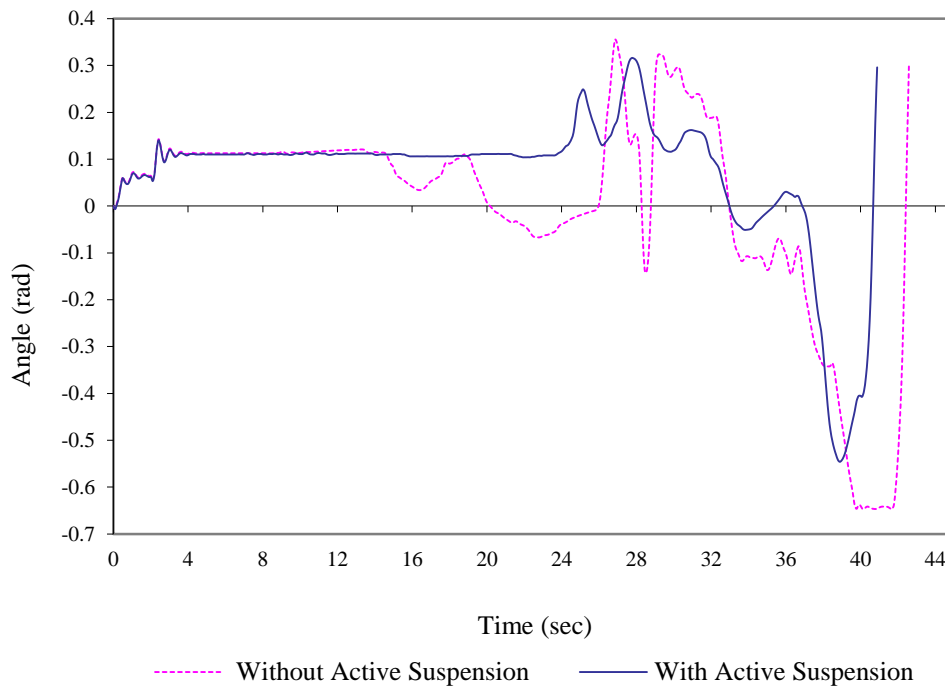


Figure 12: Sprung mass roll angle with and without active suspension Toyota Chevrolet S-10, Pickup #1.

Figures 13 demonstrated that at the point of lift-off, in the model without active suspension, tire forces under the right rear (RR) and right front (RF) tires went to zero. When the same tires were evaluated in models with active suspension, however, it was found that some tire forces remained (Figure 14). This residual force prevented lift-off.

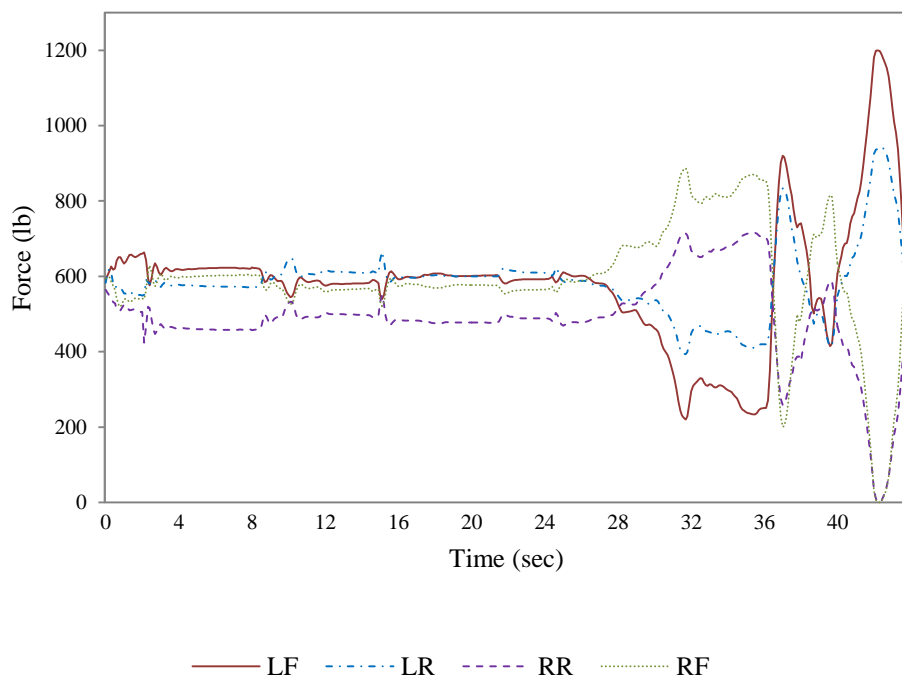


Figure 13 Left Rear (LR), Left Front (LF), Right Rear (RR), and Right Front (RF) tire forces without active suspension, Chevrolet S-10, Pickup #1.

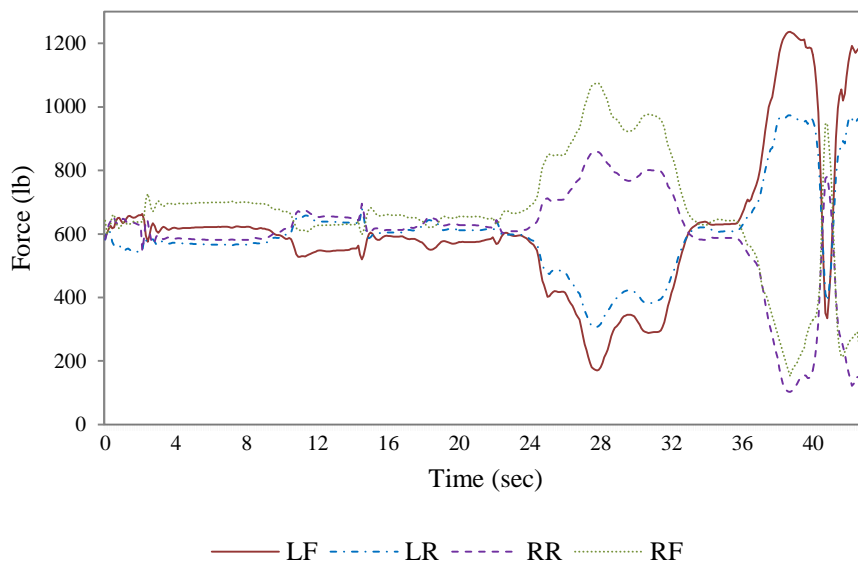


Figure 14: Left Rear (LR), Left Front (LF), Right Rear (RR), and Right Front (RF) tire forces with active suspension, Chevrolet S-10, Pickup #1.

Actuator forces have been illustrated in Figures 15 and 16, varying from -400 (lbs) to 250(lbs). These figures demonstrate that, with respect to standard actuator peak power, the designed active suspension performance can be achieved using the normal hydraulic actuator preferred in the industry.

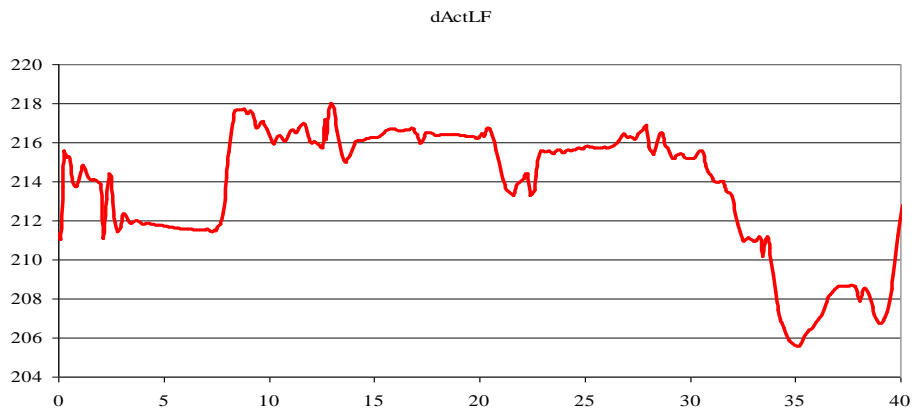


Figure 15: Actuator force - Left-Front tire force Ford Taurus 4-Dr, Passenger Car #1.

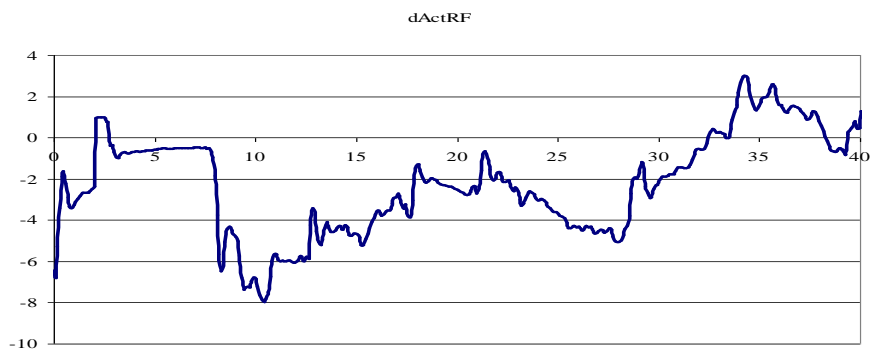


Figure 16: Actuator force - Right-Front tire force Ford Taurus 4-Dr, Passenger Car #1.

A frequency-response approach to the analysis and design of the control system is presented next. Figure 17 shows the frequency response of a "body roll angle= Y1, body roll acceleration=Y2, Right Front Suspension Force=U1, Left Front

Suspension Force=U2, Right Rear Suspension Force=U3, and Left Rear Suspension Force=U4". The LQRY controller is designed to reduce roll angle and roll velocity. The performance of the LQRY controller has shown good result at minimizing the roll angle in frequencies between 4-20 rad/sec. In roll velocity (third and fourth row of the Figure 17), however, LQRY's performance is not as strong.

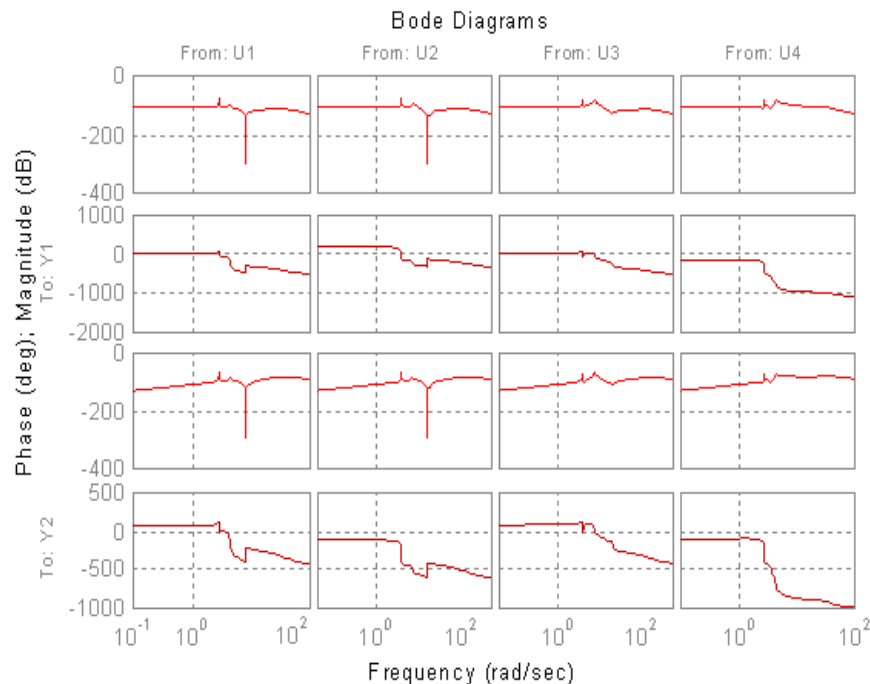


Figure 17: Bode diagrams of the active suspension system with full vehicle model.

X. CONCLUSIONS

This paper outlines the process of designing an active suspension system which uses actuator forces to create a balance in a vehicle's tire forces. This action reduces the possibility of rollover occurrence because it prevents lift-off, the predominant cause of rollovers. The steps conducted in this research, to achieve the active suspension system design were begun with creating a visual basic module. In LQRY controller design, roll angle and roll velocity are considered while other factors such as vertical displacement and acceleration are neglected. This module was then added to the VDNAL suspension breakpoint. It was then necessary to create an interface between the active suspension module and the vehicle dynamic model. Tire forces were then calculated for each time cycle.

Actuator forces with visual basic active suspension programs were also calculated for each individual time cycle. Finally, two measured forces were added as the new tire force. Once all these steps were accomplished, the new active suspension system was in place.

Although a designer may not be certain of the performance of any of the given neglected factors, it was found that using the LQRY technique overall performance of the system may be improved.

REFERENCES

- [1] T. Gillespie, Fundamentals Vehicle Dynamics, Chapter 9, pp.241.
- [2] E. Esmailzadeh and H. Taghirad, Active Vehicle Suspensions with Optimal State-Feedback Control, Int. Journal of Modeling and Simulation, Vol.18, No. 3, 1998.
- [3] Mohammad Biglarbegiana, William Meleka & Farid Golnaraghi, Vehicle System Dynamics: International Journal of Vehicle Mechanics and Mobility Volume 46, Issue 8, pp.691-711, 2008
- [4] M. Crosby and D. Karnopp, The Active Damper, Shock and Vibration Bulletin, 1973.
- [5] J. Hedrick, and, D. Wormley, Active Suspension for Ground Transport Vehicles – A State of the Art Review, Mechanics of Transportation Suspension Systems, ASME, AMD-Vol. 15, pp.21-40, 1975

- [6] Mahmoud El-Kafafy, Samir M. El-Demerdash, Al-Adl Mohamed Rabeih , Automotive Ride Comfort Control Using MR Fluid Damper, *Vehicle System Dynamics* Vol.4 No.4, PP. 179-187, April 2012.
- [7] D. Karnopp, Theoretical Limitation in Active Vehicle Suspension, *Vehicle System Dynamics*, 2006.
- [8] A. Thompson, An Active Suspension with Optimal Linear State Feedback, *Vehicle System Dynamics*, 1976.
- [9] A. Thompson, and C. Pearce., An Optimal Suspension for An Automobile on A Random Road, SAE, 790478, 1979.
- [10] J. Hedrick., Railway Vehicle Active Suspension, *Vehicle System Dynamics*, pp.267-283, 1980.
- [11] R. Goodall and W. Kortu, Active Control in Ground Transportation–A Review of the State-of-the-Art and Future Potential, *Vehicle System Dynamics*, Vol.12, pp.225-257, 1983.
- [12] R. Goodall, R. Williams, and A. Lawton, Practical Applications of Active Controlled Suspensions to Railway Vehicles, ASME, New York, 1979.
- [13] E. Bender, D.Karnopp, and I. L. Paul, On the Optimization of Vehicle Suspensions Using Random Process theory, ASME Paper No. 67-Trans12, 1967.
- [14] J. Hedrick and Alleyne, Nonlinear Adaptive Control of Active Suspensions, *IEEE Trans. Control System Technology*, Vol.3, pp.94-101, 1995.
- [15] C. Yue., T. Butsuen, and Hedrick, Alternative Control Laws for Automotive Active Suspensions, *ASME Journal of Dynamics Systems, Measurement, and Control*, Vol.111, pp. 286-291, 1989.
- [16] E. Abdellahi, D. Mehci, and M. Saad, On The Design of Active Suspension System by H^∞ and Mixed H^2/H^∞ : an LMI Approach, *IEEE, Proceeding of the American Control Conference*, pp. 4041-4045.
- [17] D. Williams and W. Haddad, Nonlinear Control of Roll Moment Distribution to Influence Vehicle Yaw Characteristics, *IEEE Transactions on Control Systems Technology*, Vol.3, No.1, pp.110-116, 1995.
- [18] R. Chalasani, Ride Performance Potential of Active Suspension System–Part II: Comprehensive Analysis Based on a Full-Car Model, *Symposium on Simulation and Control of Ground Vehicles and Transportation Systems*, Vol.80, DSC-Vol.2, ASME, 1986.
- [19] R. Chalasani, Ride Performance Potential of Active Suspension System–Part I: Simplified Analysis Based on a Quarter-Car Model, *Symposium on Simulation and Control of Ground Vehicles and Transportation Systems*, Vol.80, DSC-Vol.2, ASME, 1986.
- [20] H. Taghirad and Esmailzadeh, Vehicle Suspension Systems Control: A Review, *INTERNATIONAL JOURNAL OF CONTROL, AUTOMATION AND SYSTEMS*, Vol.2, No 2, pp. 46-54, 2013.
- [21] J. Lin. and I. Kanellakopoulos, Nonlinear Design of Active Suspension, *IEEE Control System Magazine*, Vol.17, pp.45-59, 1997.
- [22] H. Hashemipour, Nonlinear Optimal Control of Vehicle Active Suspension Considering Actuator Dynamics, *International Journal of Machine Learning and Computing*, Vol. 2, No. 4, August 2012.
- [23] T. Yoshimura, K. Nakaminami, M. Kurimoto., and J. Hino, Active Suspension of Passengers Cars Using Linear and Fuzzy-Logic Control, *Control Engineering Practice*, Vol.7, pp. 4147, 1999.
- [24] S. Ikenga, L. Lewis, J. Campos and L. Davis, Active Suspension Control of Ground Vehicle Based on a Full-Vehicle Model.
- [25] T. Wielenga, A Method for Reducing On-Road Rollovers – Anti-Rollover Braking, SAE SP-1445, 2011.
- [26] S Ehsan Razavi, Javad Royaei, Mehdi Bahadorzadeh, Design a low current and high-speed shift register based on D type flip flop, 2015 Forth International Conference on e-Technologies and Networks for Development (ICeND), Pages 1-4, IEEE September. 2015.
- [27] A. Talebpour, H. Mahmassani, and S. Hamdar, Modeling Lane-Changing Behavior in a Connected Environment: A Game Theory Approach, *Transportation Research Procedia*, Volume 7, pp. 420-440, 2015.
- [28] P Rad, M Nikdadian, M Bahadorzadeh, Synchronizing the fractional-order Genesio-Tesi chaotic system using adaptive control, *Int J Sci Eng Res*, Vol. 6, Pages 1699-1702

APPENDIX A

IMPLEMENTING ACTIVE SUSPENSION MODULE TO THE VDANL PROGRAM (Break Point)

=====

VDANL Suspension Parameters' Definitions

VehicleNum - Indicates vehicle type:

T - Current simulation time (Single precision)

DT - Current simulation update rate (Single precision)

V - Main Vehicle parameters (VehicleParams)

V2 - Attached vehicle parameters: if VehicleNum = 1, then V2

will be the trailer, if VehicleNum = 2, then V2 will be the
tow vehicle (VehicleParams)

TIRE - Tire Parameters (TireParams)

NL - NONLIN.PAR Parameters (NonLinParams)

VD - Vehicle Dynamic variables if VehicleNum = 1, then VD
will be the tow vehicle, if VehicleNum = 2, then VD will be
the trailer (VehicleParams)

WT - Wheel and Tire dynamic variables (WheelDynamics)

TM - Terrain Model variables (TerrainModel)

RC - Run Control variables (RunControl)

VDANLUI - VDANL User Interface data (VDANLUserInterface)

UM - User Module output data (UMData)

=====

Dimension local variables

Dim nFile As Long

Dim dActLF As Double

Dim dActLR As Double

Dim dActRF As Double

Dim dActRR As Double

If T >= LastTime + 0.1 Then

nFile = FreeFile

If T < 0.01 Then

sFile = "c:\code\hamed\suspension\out" & Format(Now, "MMDDHHMM") & ".txt"

End If

=====

Printing Output Data

Open sFile For Append As #nFile

Print #nFile, "SimTime" & vbTab & T & vbTab & "FSLF" & vbTab & VD.FSLF & vbTab & "FSLR" & vbTab &
VD.FSLR & vbTab & "FSRR" & vbTab & VD.FSRR & vbTab & "FSRF" & vbTab & VD.FSRF & vbTab & vbTab &
"Roll" & vbTab & VD.PHIS & vbTab & "RollV" & vbTab & VD.PHISD

Close #nFile

LastTime = T

End If

Actuator Forces

dActLF: Actuator Force for Left Front Tire

dActRF: Actuator Force for Right Front Tire

dActLR: Actuator Force for Left Rear Tire

dActRR: Actuator Force for Right Rear Tire

$$\begin{aligned} \mathbf{dActLF} = & (V.HS - VD.ZS) * 3.2808 * -1 * 0.1071 + VD.ZSD * 3.2808 * 0.1321 + VD.The * -1 * 0.2789 + \\ & VD.THED * -1 * 0.0552 + VD.PHIS * 1.2351 + VD.PHISD * 0.0716 + (Tire(1).RR - VD.ZSLF) * 3.2808 * -1 * 0.0001 \\ & + VD.ZSLFD * 3.2808 * -1 * 0.0146 + (Tire(2).RR - VD.ZSRF) * 3.2808 * -1 * 0.001 + VD.ZSRFD * 3.2808 * -1 * \\ & 0.0013 + (Tire(3).RR - VD.ZSLR) * 3.2808 * -1 * 0.0135 + VD.ZSLRD * 3.2808 * 0.011 + (Tire(4).RR - VD.ZSRR) * \\ & 3.2808 * -1 * 0.3442 + VD.ZSRRD * 3.2808 * -1 * 0.0146 \end{aligned}$$

$$\begin{aligned} \mathbf{dActRF} = & (V.HS - VD.ZS) * 3.2808 * -1 * 0.1074 + VD.ZSD * 3.2808 * 0.0002 + VD.The * -1 * 0.0764 + \\ & VD.THED * -1 * 0.214 + VD.PHIS * -1 * 1.3431 + VD.PHISD * -1 * 0.0861 + (Tire(1).RR - VD.ZSLF) * 3.2808 * -1 * \\ & 0.0387 + VD.ZSLFD * 3.2808 * -1 * 0.0032 + (Tire(2).RR - VD.ZSRF) * 3.2808 * 1 * 0.0067 + VD.ZSRFD * 3.2808 * \\ & 1 * 0.0184 + (Tire(3).RR - VD.ZSLR) * 3.2808 * -1 * 0.0188 + VD.ZSLRD * 3.2808 * -1 * 0.0198 + (Tire(4).RR - \\ & VD.ZSRR) * 3.2808 * 1 * 0.4377 + VD.ZSRRD * 3.2808 * -1 * 0.0003 \end{aligned}$$

$$\begin{aligned} \mathbf{dActLR} = & (V.HS - VD.ZS) * 3.2808 * 1 * 0.5793 + VD.ZSD * 3.2808 * 0.3909 + VD.The * 1 * 0.6541 + \\ & VD.THED * 1 * 0.6706 + VD.PHIS * 1.3925 + VD.PHISD * 0.1591 + (Tire(1).RR - VD.ZSLF) * 3.2808 * 1 * 0.0298 + \\ & VD.ZSLFD * 3.2808 * 1 * 0.015 + (Tire(2).RR - VD.ZSRF) * 3.2808 * 1 * 0.002 + VD.ZSRFD * 3.2808 * -1 * 0.0342 + \\ & (Tire(3).RR - VD.ZSLR) * 3.2808 * -1 * 0.0035 + VD.ZSLRD * 3.2808 * 0.0661 + (Tire(4).RR - VD.ZSRR) * 3.2808 * \\ & -1 * 0.9877 + VD.ZSRRD * 3.2808 * 1 * 0.0198 \end{aligned}$$

$$\begin{aligned} \mathbf{dActRR} = & (V.HS - VD.ZS) * 3.2808 * -1 * 0.4563 + VD.ZSD * 3.2808 * 0.3072 + VD.The * -1 * 1.0482 + \\ & VD.THED * 1 * 0.4793 + VD.PHIS * -1 * 3.4802 + VD.PHISD * -1 * 0.0752 + (Tire(1).RR - VD.ZSLF) * 3.2808 * -1 * \\ & 0.3722 + VD.ZSLFD * 3.2808 * -1 * 0.0137 + (Tire(2).RR - VD.ZSRF) * 3.2808 * 1 * 0.4314 + VD.ZSRFD * 3.2808 * \\ & 1 * 0.0013 + (Tire(3).RR - VD.ZSLR) * 3.2808 * -1 * 0.5078 + VD.ZSLRD * 3.2808 * 0.0238 + (Tire(4).RR - \\ & VD.ZSRR) * 3.2808 * 1 * 0.1635 + VD.ZSRRD * 3.2808 * 1 * 0.0167 \end{aligned}$$

Modified Tire Force after New Actuator Forces

$$VD.FSLF = VD.FSLF + dActLF$$

$$VD.FSRF = VD.FSRF + dActRF$$

$$VD.FSLR = VD.FSLR + dActLR$$

$$VD.FSRR = VD.FSRR + dActRR$$

End Function